NASA TECHNICAL NOTE

NASA TN D-7625

NASA TN D-7625

TURBINE FOR A LOW-COST TURBOJET ENGINE

I - Design and Cold-Air Performance

by Milton G. Kofskey, Richard J. Roelke, and Jeffrey E. Haas

Lewis Research Center
and
U.S. Army Air Mobility R&D Laboratory
Cleveland, Ohio 44135

NATIONAL AERONAUTICS AND SPACE ADMINISTRATION • WASHINGTON, D. C. • JUNE 1974

1. Report No.	2. Government Accession No.	3. Recipient's Catalog No.
NASA TN D-7625		

4. Title and Subtitle	5. Report Date
TURBINE FOR A LOW-COST TURBOJET ENGINE I - DESIGN AND COLD-AIR PERFORMANCE	June 1974
	6. Performing Organization Code
7. Author(s) Milton G. Kofskey, Richard J. Roelke, and Jeffrey E. Haas	8. Performing Organization Report No. E-7754
	10. Work Unit No. 501-24
9. Performing Organization Name and Address NASA Lewis Research Center and U.S. Army Air Mobility R&D Laboratory Cleveland, Ohio 44135	11. Contract or Grant No.
	13. Type of Report and Period Covered Technical Note
12. Sponsoring Agency Name and Address National Aeronautics and Space Administration Washington, D.C. 20546	14. Sponsoring Agency Code

15. Supplementary Notes

16. Abstract

A 24.70-cm (9.72-in.) tip diameter single-stage, axial-flow turbine was designed for a turbojet engine. Cold-air tests were made over a range of speeds from 30 to 105 percent of design equivalent speed and over a range of total-pressure ratios from 1.30 to 2.66. Results are presented in terms of specific work, torque, mass flow, and efficiency.

17. Key Words (Suggested by Author(s))	18. Distribution Statement
Axial-flow turbine; Single-stage turbine; Gas turbine; Efficiency; Performance tests	Unclassified - unlimited Category 28

19. Security Classif. (of this report)	20. Security Classif. (of this page)	21. No. of Pages	22. Price*
Unclassified	Unclassified	20	$3.00

* For sale by the National Technical Information Service, Springfield, Virginia 22151

TURBINE FOR A LOW-COST TURBOJET ENGINE

I - DESIGN AND COLD-AIR PERFORMANCE

by Milton G. Kofskey, Richard J. Roelke, and Jeffrey E. Haas

Lewis Research Center and
U.S. Army Air Mobility R&D Laboratory

SUMMARY

An experimental investigation of a singel-stage, 24.70-centimeter (9.72-in.) tip diameter axial-flow turbine was made to determine the performance over a range of speed and pressure ratio. Cold-air tests were made at speeds from 30 to 105 percent of design equivalent speed and total pressure ratios from 1.30 to 2.66.

The results of the investigation indicated total and static efficiencies of 0.91 and 0.79, respectively, at design-point operation. The total efficiency is substantially higher than the 0.88 assumed in the design. This higher efficiency would not necessarily be obtained by the turbine in actual hot engine operation. Losses due to nonuniform turbine-inlet conditions, stator-hub leakage and increased rotor-tip clearance obtained in engine operation were estimated to result in 3.5 points in efficiency. A rating efficiency of 0.90 was obtained at design-point operation in the turbine component tests. The difference between total and rating efficiencies indicates that the exit-whirl loss amounted to 1 point in efficiency at design-point operation.

The equivalent mass flow was 2.27 kilograms per second (5.00 lb/sec) at design equivalent speed and design total-pressure ratio of 1.909. This mass flow was 9.5 percent smaller than design value. This deficiency in mass flow was the result of the stator-throat area being 9.4 percent smaller than that required for design mass flow.

INTRODUCTION

One of the major problems in the use of gas turbine engines for civilian single and twin engine light planes is the high cost of the engine. Studies (refs. 1 and 2) have been made at the Lewis Research Center for achieving cost reductions on the gas turbine engine. To achieve lower cost, a moderate turbine-inlet temperature was selected for

reliability as well as for its allowance of the use of low-cost materials. The studies have been made for both a fan-jet and a turbojet engine. These engines were designed for a flight Mach number of 0.65 at an altitude of 7620 meters (25 000 ft). The turbine for the fan-jet engine was designed and fabricated for a cold-air performance evaluation. The results of the performance evaluation are given in references 3 and 4.

A turbine for the turbojet engine was also designed. This engine is of interest for general aviation as well as such military applications as drones, missiles, and various remotely piloted vehicles. A model of the turbine was built and tested in a cold air facility. Each blade row, stator and rotor, was an integral casting. The cold test conditions included an inlet temperature of 310 K (560° R) and a pressure of 10.8 newtons per square centimeter (15.7 psia). The turbine was operated at speeds from 30 to 105 percent of the equivalent design speed and pressure ratios from 1.30 to 2.66.

This report includes design and experimental performance information about the turbine. Performance results are presented in terms of equivalent torque, equivalent mass flow, equivalent work, efficiency, and rotor-exit flow angle.

SYMBOLS

Δh specific work, J/g; Btu/lb

N turbine speed, rpm

p pressure, N/cm^2 abs; psia

T absolute temperature, K; $^{\circ}R$

U blade velocity, m/sec; ft/sec

V absolute gas velocity, m/sec; ft/sec

W relative gas velocity, m/sec; ft/sec

w mass flow, kg/sec; lb/sec

α absolute gas flow angle measured from axial direction, deg

β relative gas flow angle measured from axial direction, deg

γ ratio of specific heats

δ ratio of inlet total pressure to U.S. standard sea-level pressure, p_1'/p^*

ϵ function of γ used in relating parameters to those using air inlet conditions at U.S. standard sea-level conditions, $(0.740/\gamma)[(\gamma + 1)/2]^{\gamma/(\gamma-1)}$

η_s static efficiency: ratio of turbine work based on torque, mass flow, and speed measurements to ideal work based on inlet total temperature and inlet total and exit static pressure

η_t total efficiency: ratio of turbine work based on torque, mass flow, and speed measurements to ideal work based on inlet total temperature and inlet and exit total pressure

η_x rating efficiency: ratio of turbine work based on torque, mass flow, and speed measurements to ideal work based on inlet total temperature and inlet and exit total pressure, both defined as sum of static pressure plus pressure corresponding to calculated average axial component of velocity

θ_{cr} squared ratio of critical velocity at turbine inlet to critical velocity at U.S. standard sea-level air, $(V_{cr}/V^*_{cr})^2$

τ torque, N-m; ft-lb

ω turbine speed, rad/sec

Subscripts:

cr condition corresponding to Mach number of unity

eq equivalent

m mean radius

t tip

1 measuring station at turbine inlet (fig. 4)

2 measuring station at stator exit (fig. 4)

3 measuring station at rotor exit (fig. 4)

Superscripts:

' absolute total state

* U.S. standard sea-level conditions (temperature equal to 288.2 K (518.7° R), pressure equal to 10.13 N/cm^2 (14.70 psia))

TURBINE DESIGN

The turbine was designed for a low-cost civilian turbojet engine. This design section presents the design requirements and physical characteristics of the scaled turbine.

The turbine design conditions are listed in table I, and the design velocity diagrams are given in figure 1. The single-stage, axial-flow turbine includes a free-vortex whirl

distribution. As can be noted from the work factor value and the velocity diagrams, the machine is a conservative aerodynamic design, operating with moderate gas temperatures.

Also listed in table I are the equivalent operating conditions of the engine turbine. Note that all of the equivalent conditions listed would not be exactly obtained in a cold-air component test. The component test hardware and engine hardware would have some physical differences. Cross sections of the engine turbine and test turbine are shown in figures 2 and 3, respectively. Changes made in the test hardware were the elimination of the rotor labyrinth seal and a decrease in the rotor-tip clearance. Also, even with identical cold blading in the component test rig and engine, the engine turbine will expand thermally at engine operating temperatures.

The calculated thermal expansion would increase the turbine flow area by about 2.5 percent. Therefore, the equivalent flow rate in the component rig is expected to be about 98 percent of the engine flow rate, or 2.457 kilograms per second (5.416 lb/sec). The turbine efficiency is expected to be higher in the component rig for a number of reasons. The blade tip clearance in the component rig was 0.28 millimeter (0.011 in.); in the engine the design clearance was 0.79 millimeter (0.031 in.). Also, hub-labyrinth-leakage flow in the engine turbine, as well as turbine-inlet temperature gradients, are not present in the component rig. The effects of these differences, based in part on test data from other turbine investigations, have been estimated and are as follows:

Engine turbine efficiency	0.88
Rotor tip clearance effect	0.03
Inlet temperature gradient and hub leakage	0.005
Component rig efficiency	0.915

Selected blading information is given in table II. The solidity listed is based on axial chord. Stator and rotor profiles and passages are shown in figure 4. Both stator and rotor have changing cross sections and blade twist from hub to tip. The blade surface velocities at the mean sections (fig. 5) were computed for the engine design condition. However, no adverse channel flow was indicated for the new operating condition. A photograph of the turbine rotor is shown in figure 6.

APPARATUS

The apparatus consisted of the turbine, a cradled gearbox, and a cradled dynamometer to absorb the power output of the turbine and to control turbine speed. In addition, there was inlet and exhaust piping with flow controls for setting inlet and exit pressures

of the turbine. The arrangement of the apparatus is shown schematically in figure 7(a). High-pressure dry air was supplied from the laboratory air system. The air passed through a filter, through a mass-flow measuring station (consisting of a calibrated flat-plate orifice), through a remotely controlled turbine-inlet valve, through an inlet plenum, and into the turbine. After going through the turbine, the air was exhausted through a system of piping and a remotely operated valve into the laboratory low-pressure exhaust system. A 224-kilowatt (300-hp) dynamometer cradled on hydrostatic bearings was used to absorb the turbine power, control speed, and measure torque. The dynamometer was coupled to the turbine shafting through a gearbox cradled on hydrostatic bearings. The gearbox provided relative rotative speeds between dynamometer and turbine of 1.0 to 8.50. The stators of the gearbox and dynamometer were coupled together so that the measured torque was that developed by the turbine. Figure 7(b) shows the turbine installed in the test facility.

INSTRUMENTATION

A torque arm attached to the dynamometer stator transmitted the turbine torque to a commercial strain-gage load cell. This electric signal was sent to the digital voltmeter equipment. The rotational speed was detected by a magnetic pickup and a shaft-mounted gear. The signal was converted to a direct-current voltage and fed into the digital voltmeter.

Turbine performance was determined by measurements taken at the stator inlet and at the rotor exit. The instrumentation stations are shown in figure 4. The instrumentation at the turbine inlet (station 1) was located approximately one axial mean-chord length upstream of the stator blades and included three static-pressure taps equally spaced circumferentially on both the inner and outer walls. Also, three total-temperature rakes, each containing three thermocouples, were located in the same axial plane. There were three static-pressure taps, equally spaced circumferentially at the hub and tip of the stator exit (station 2). The tip static taps were located midway between two adjacent blades and in a plane just downstream of the stator-blade trailing edge. The axial length of the stator hub shroud was smaller than design, hence the stator-hub static-pressure taps were located just inside the stator passage and midway between two adjacent blades. These are of questionable value in obtaining free-stream conditions at the hub.

At station 3, located approximately one axial mean-chord length downstream of the rotor exit, there were six static-pressure taps equally spaced circumferentially (three each at the inner and outer walls). The outlet flow angle was measured with an angle sensitive probe and a self-alining probe actuator. The values of the pressures at the various stations were measured by unbonded, strain-gage transducers. A 200-channel

data-acquisition system was used to measure and record the electrical signals from the pressure transducers as well as the temperature readouts.

PROCEDURE

Data were obtained at nominal inlet total conditions of 310 K (560° R) and 10.82 newtons per square centimeter (15.7 psia). Data were obtained over a range of equivalent inlet-total to exit-total pressure ratio from 1.30 to 2.66 and a speed range from 30 to 105 percent of equivalent design.

Dynamometer-torque calibrations were obtained before and after each daily series of runs. An average of these two calibrations was then used in the calculation of turbine work output. The torque calibrations were obtained without the dynamometer rotating, and thus the effects of turbine bearing and friction are included in the turbine work.

The turbine was rated on the basis of total efficiency η_t and static efficiency η_s over the range of pressure ratio and speeds investigated. The turbine was also rated on a rating efficiency η_x at equivalent design speed and over a range of pressure ratios, which is based on the exit total pressure determined from the axial component. This calculated value of turbine-exit-total-pressure charges the turbine for the energy of the whirl component existent in the leaving velocity of the gas. All total pressures were calculated from mass flow, total temperature, static pressure, and flow angle. The total temperature at the turbine exit was calculated using the measured inlet-total temperature and the calculated overall turbine work output. In the calculation of turbine-inlet total pressure, the flow angle was assumed to be zero.

RESULTS AND DISCUSSION

Performance results are presented for a 24.70-centimeter (9.72-in.) tip-diameter single-stage axial-flow turbine suitable for missile or drone applications. Performance tests were made with air as the working fluid at total inlet conditions of 310 K (560° R) and 10.82 newtons per square centimeters (15.70 psia). The turbine was operated over a range of rotative speeds from 30 to 105 percent of equivalent design and over a range of total-pressure ratio from 1.30 to 2.66. Experimental results include overall performance in terms of equivalent mass flow, equivalent torque, equivalent specific work, and efficiency. Included are variations of turbine-outlet flow angle and stator outlet tip static-pressure variation with speed and turbine pressure ratio.

Mass Flow

Figure 8 shows the variation of equivalent mass flow with total-pressure ratio and speed. An equivalent mass flow of 2.27 kilograms per second (5.00 lb/sec) was obtained at equivalent design speed and at the design total-pressure ratio of 1.909. This mass flow is 9.5 percent smaller than the design value of 2.507 kilograms per second (5.527 lb/sec) for hot operation. Before the tests, measurements indicated that the stator throat area was 6.4 percent smaller than the design throat area because of manufacturing errors and cold testing. A flow check of the stator, without the rotor in place and at the design total- to static-pressure ratio, indicated that the mass flow was about 9.5 percent of the design value for hot operation. Therefore, it can be concluded that even if the stator had been built according to specifications, the design stator throat area of the ordnance turbine would have been about 3 percent undersize.

At equivalent design speed, a choking mass flow of 2.30 kilograms per second (5.07 lb/sec) was obtained. Since there is no observable variation of choking mass flow with speed, the stator is choked and, therefore, controls the flow through the turbine.

Equivalent Torque

Figure 9 shows the variation of equivalent torque with total-pressure ratio for lines of constant speed. An equivalent torque value of 52.6 newton meters (38.8 ft-lb) was obtained at equivalent design speed and design total-pressure ratio of 1.909. This is about 8.1 percent smaller than design. This lower torque value is primarily the result of the mass flow being 9.5 smaller than design. Since the torque was 8.1 percent smaller than design and the mass flow 9.5 percent smaller than design, it is apparent that the turbine total efficiency would be higher than the 0.88 assumed in the design. The torque curves show that limiting load was not reached even though pressure ratios considerably higher than design were obtained.

Rotor Exit Flow Angle

Figure 10 shows the variation of rotor-exit flow angle as a function of pressure ratio for lines of constant equivalent speed. The flow angles were measured at the mean radius and from the axial direction. Negative angles indicate a positive contribution to specific work. At design equivalent speed and pressure ratio of 1.909, the exit flow angle was about $+14^{\circ}$. The velocity diagram of figure 1 shows that the original turbine was designed for a mean-radius exit-flow angle of -3.8° at a work factor of 1.282. At

design speed the turbine operates at a work factor of 1.282 at a total-pressure ratio of 2.057. The exit angle at this work factor is about $+6.0^{\circ}$. Increased rotor inlet whirl, due to overexpansion of the stator as a result of the smaller throat area, could account for some of the difference from $+6.0^{\circ}$ to -3.8°.

Turbine Efficiency

A performance map for the subject turbine is shown in figure 11. The map shows equivalent specific work output $\Delta h/\theta_{cr}$ as a function of the mass-flow - speed parameter $\epsilon\omega w/\delta$ for the various equivalent speeds investigated. Lines of constant pressure ratio and efficiency are superimposed. Figure 11(a) shows the performance of the turbine based on total conditions across the turbine. A total efficiency of 0.91 was obtained at the equivalent design speed and total-pressure ratio. This is 3 percentage points higher than the 0.88 assumed in the design. Although the experimental total efficiency was significantly higher than design, this higher efficiency would not necessarily be expected in actual hot engine operation. Losses due to nonuniform turbine inlet conditions, stator hub leakage, and increased tip clearances could result in an efficiency closer to the design value than that obtained in this cold-air investigation. As indicated in the TURBINE DESIGN section, these losses were estimated to amount to 3.5 percentage points in efficiency.

Over the range of pressure ratio and speeds investigated, the total efficiency varied from about 0.60 near the 30-percent speed line to over 0.91 in the 100- and 105-percent speed lines. The speed lines indicate that the flow chokes at decreasing pressure ratios as the speed was decreased from the 105 percent value.

Figure 11(b) shows the performance map when based on inlet-total- to exit-static-pressure ratio. At the condition corresponding to design equivalent speed and total-pressure ratio, the total- to static-pressure ratio was 2.136. At this operating point the static efficiency was slightly over 0.79. Since the total efficiency was 0.91 for this operating point, there was 12 percentage points in efficiency due to rotor exit kinetic energy.

Over the range of pressure ratio and speeds investigated, the static efficiency varied from 0.40 near the 30-percent speed line to slightly over 0.79 for the 90, 100, and 105 percent speed lines.

Figure 12 is a comparison of the total η_t and rating η_x efficiencies for equivalent design speed and over the range of total-pressure ratio investigated. The rating efficiency was 0.90 at the design-point pressure ratio, which indicates an exit-whirl loss of 1 percentage point in efficiency. Note that the total and rating efficiencies are at the same value (0.91) at the pressure ratio of about 2.18. This results because the absolute rotor-exit flow angle is axial at the pressure ratio of 2.18 (fig. 10).

The separation of the two efficiency curves for pressure ratios other than the 2.18 value is the result of the variation of rotor-exit flow angle with pressure ratio.

Static-Pressure Distribution

Figure 13 shows the variation of stator-exit-tip static-pressure with turbine inlet-total to exit-static-pressure ratio for lines of constant equivalent speed. The curves indicate that for a given turbine pressure ratio, stator-tip reaction increases with decreasing rotative speed. There is a corresponding decrease in rotor-tip reaction with decreasing rotative speed. The flatness of the curves at the higher pressure ratios indicate that the rotor was choked at the tip section.

Stator-exit-hub static-pressure data are not considered reliable (and are not presented) because the static taps were located slightly inside the plane tangent to the stator trailing edge. As was stated in the INSTRUMENTATION section, the axial length of the hub shroud was too short and the taps could only be placed just inside the passage. The stator hub static-pressure measurements indicated negative rotor reaction at equivalent design speed and over most of the pressure ratio range tested. It would be expected that the free-stream hub static pressure would be lower than design value at design-point operation because of over-expansion as effected by the smaller than design throat area. The measured hub static pressure would also be affected by blockage since the tap was located in the blade passage.

Figure 14 shows the variation of turbine total-pressure ratio with turbine inlet-total-to exit-static-pressure ratio for lines of constant speed. This figure was included in the report as a reference curve for the reader.

SUMMARY OF RESULTS

An experimental cold-air investigation of a single-stage axial flow turbine with a tip diameter of 24.70 centimeters (9.72 in.) was made to determine the performance over a range of speeds and pressure ratio. The turbine was designed for a turbojet engine that is suitable for general aviation and military applications. Results of the cold-air investigation may be summarized as follows:

1. An equivalent mass flow of 2.27 kilograms per second (5.00 lb/sec) was obtained at equivalent design speed and total-pressure ratio. This mass flow value is 9.5 percent smaller than the design value of 2.507 kilograms per second (5.527 lb/sec). The difference in mass flow resulted because the stator throat area was 9.4 percent smaller than that required to pass design mass flow.

2. A total efficiency of 0.91 was obtained at equivalent design speed and equivalent design total-pressure ratio. This value was 3 percentage points higher than the 0.88 assumed in the design. Although the experimental performance was significantly higher than design, additional losses due to nonuniform turbine-inlet conditions, stator hub leakage, and increased rotor tip clearance in the engine could result in efficiencies closer to the design values. These losses were estimated to result in 3.5-percentage-point decrease in total efficiency.

3. A rating efficiency of 0.90 was obtained at design equivalent speed and pressure ratio. The difference between total and rating efficiencies indicates that there was an exit-whirl loss of 1 percentage point in terms of efficiency.

4. A static efficiency of 0.79 was obtained at equivalent design speed and design total-pressure ratio. The difference between total and static efficiency at this design operating point indicated that there were 12 percentage points of efficiency tied up in kinetic energy.

Lewis Research Center,
National Aeronautics and Space Administration,
and
U.S. Army Air Mobility R&D Laboratory,
Cleveland, Ohio, December 4, 1973,
501-24.

REFERENCES

1. Cummings, Robert L.; and Gold, Harold: Concepts for Cost Reduction on Turbine Engines for General Aviation. NASA TM X-52951, 1971.

2. Cummings, Robert L.: Experience With Low Cost Jet Engines. NASA TM X-68085, 1972.

3. Kofskey, Milton G.; and Nusbaum, William J.: Design and Cold-Air Investigation of a Turbine for a Small Low-Cost Turbofan Engine. NASA TN D-6967, 1972.

4. Nusbaum, William J.; and Kofskey, Milton G.: Effect of a Reduction in Blade Thickness on Performance of a Single-Stage 20.32-Centimeter Mean-Diameter Turbine. NASA TN D-7128, 1973.

TABLE I. - TURBINE DESIGN VALUES

	Engine operation	Equivalent conditions
Inlet temperature, ^{o}K; ^{o}R	1089; 1960	288.2; 518.7
Inlet pressure, N/cm^2 abs; psia	26.34; 38.2	10.14; 14.7
Mass flow, kg/sec; lb/sec	3.28; 7.225	2.507; 5.526
Rotative speed, rpm	34 700	18 075
Specific work, J/g; Btu/lb	159.3; 68.45	43.23; 18.57
Rotor tip diameter, cm; in.	24.7; 9.72	24.7; 9.72
Energy function $\Delta h/T$, J/kg-K; Btu/lb-^{o}R	0.1463; 0.0349	0.1500; 0.0358
Speed function, $U_m/\sqrt{T}$, m/sec-K; ft/sec-^{o}R	11.26; 27.55	11.41; 27.89
Work factor, $\Delta h \times 10^3/U_m^2$	1.153	1.153
Total-to-total pressure ratio	1.862	1.909
Total efficiency, η_t	0.88	0.88

TABLE II. - SELECTED STATOR AND ROTOR PHYSICAL INFORMATION

Blading	Radius		Axial chord[a]		Solidity	Throat[a]		Number of blades
	cm	in.	cm	in.		cm	in.	
Stator	8.36	3.291	1.615	0.6358	1.076	0.5105	0.2010	35
	10.35	4.077	1.900	.7480	1.022	.7505	.2955	
	12.35	4.862	2.185	.8602	.985	1.0531	.4146	
Rotor	8.36	3.291	2.090	0.8228	2.268	0.5346	0.2105	57
	10.35	4.077	1.757	.6919	1.540	.6500	.2559	
	12.35	4.862	1.425	.5610	1.047	.7199	.2834	

[a]Hot dimensions.

Radius, cm (in.), at -			
Station 1	8.36 (3.29)	10.35 (4.08)	12.35 (4.86)
Station 2	8.36 (3.29)	10.35 (4.08)	12.35 (4.86)
Station 3	8.03 (3.16)	10.18 (4.01)	12.36 (4.87)
α_2, deg	70.0	66.0	61.4
β_2, deg	52.4	23.2	-15.7
α_3, deg	-5.8	-3.8	-3.1
β_3, deg	-53.3	-54.6	-58.0

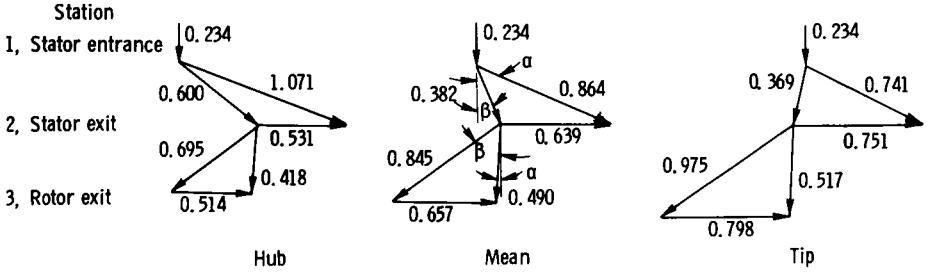

Figure 1. - Design velocity diagrams (given in terms of Mach number) for low-cost turbojet engine.

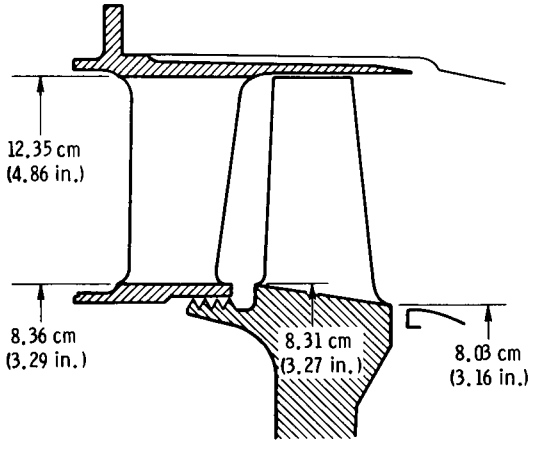

Figure 2. - Turbine meridional flowpath. Radii shown are for hot-engine conditions.

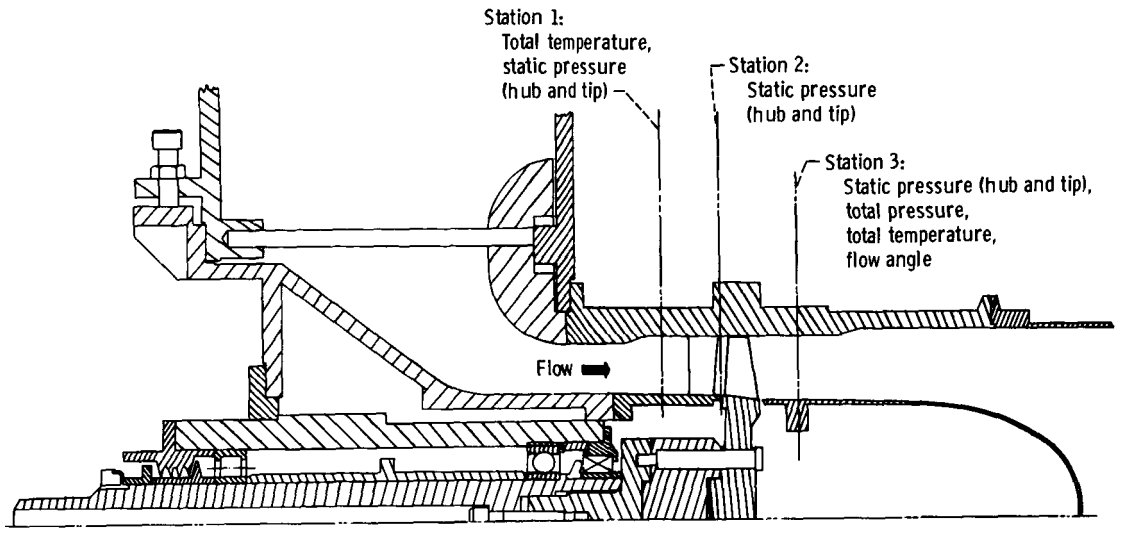

Figure 3. - Schematic of turbine for component tests.

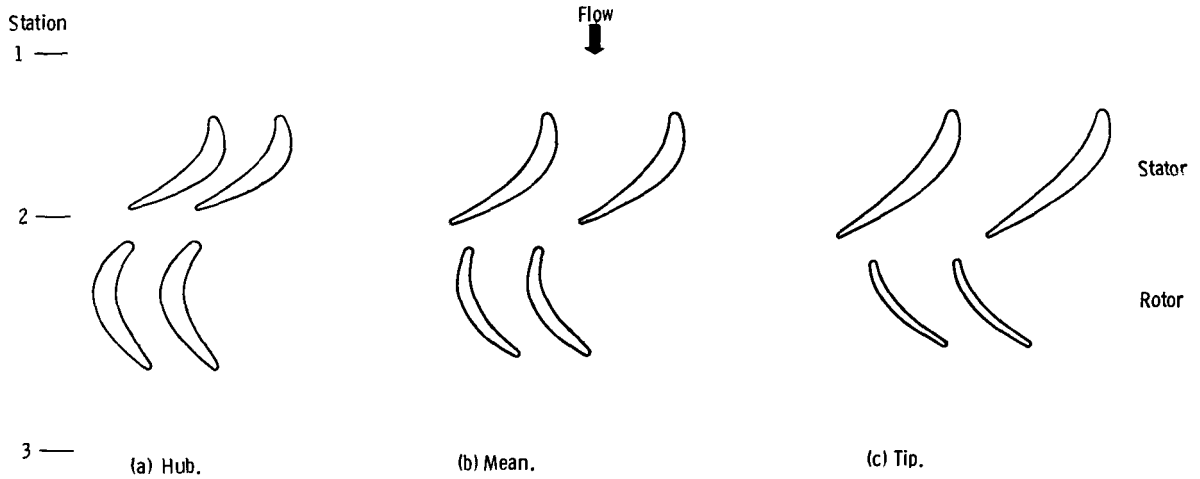

Figure 4. - Stator- and rotor-blade passages and profiles.

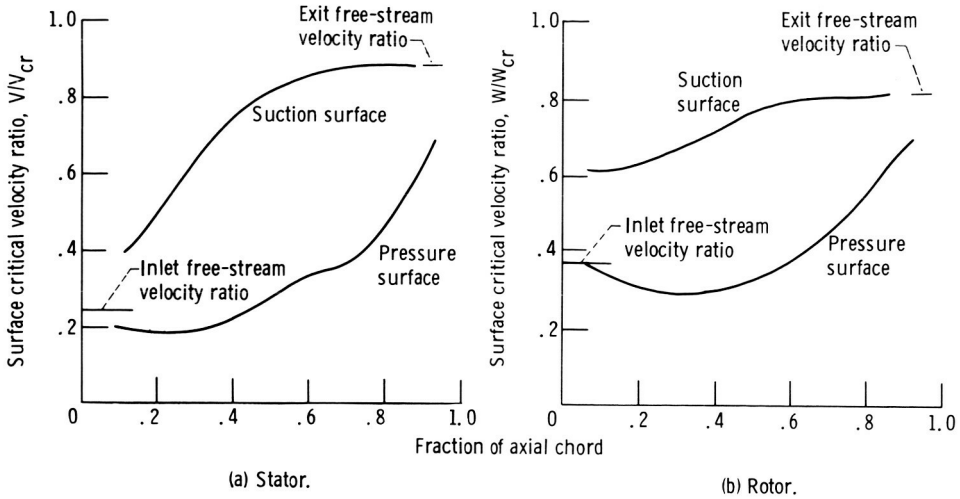

(a) Stator. (b) Rotor.

Figure 5. - Blade surface velocity distribution at mean diameter.

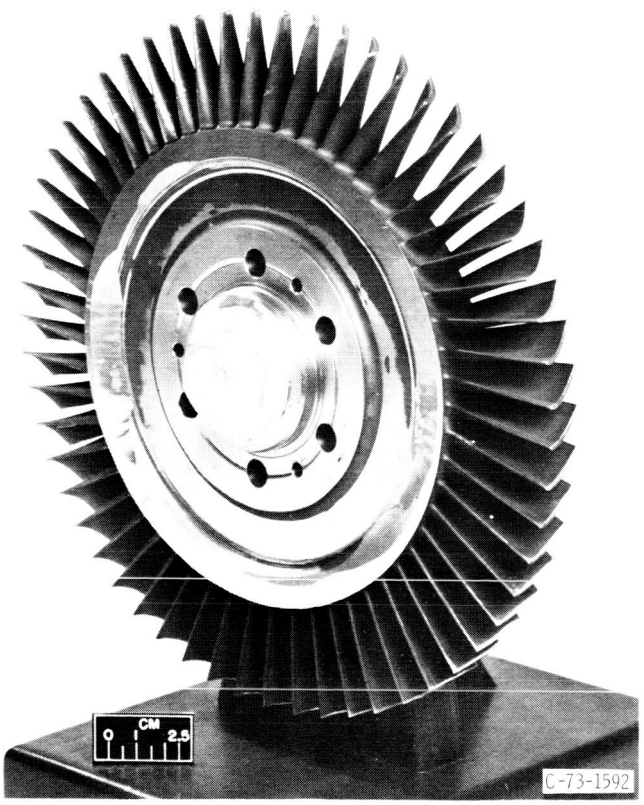

Figure 6. - Turbine rotor.

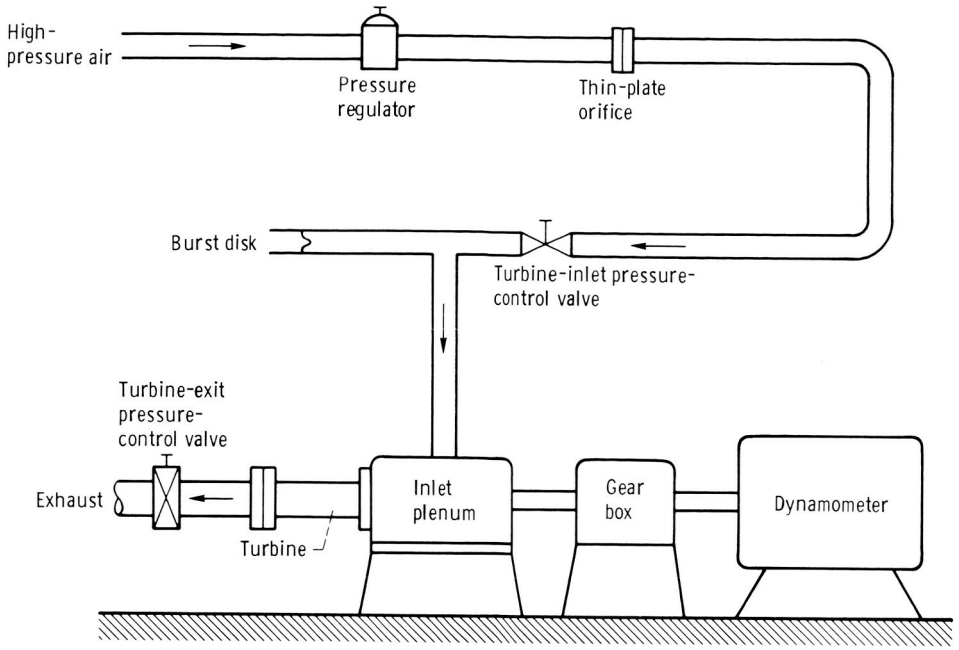

(a) Arrangement of piping and test equipment.

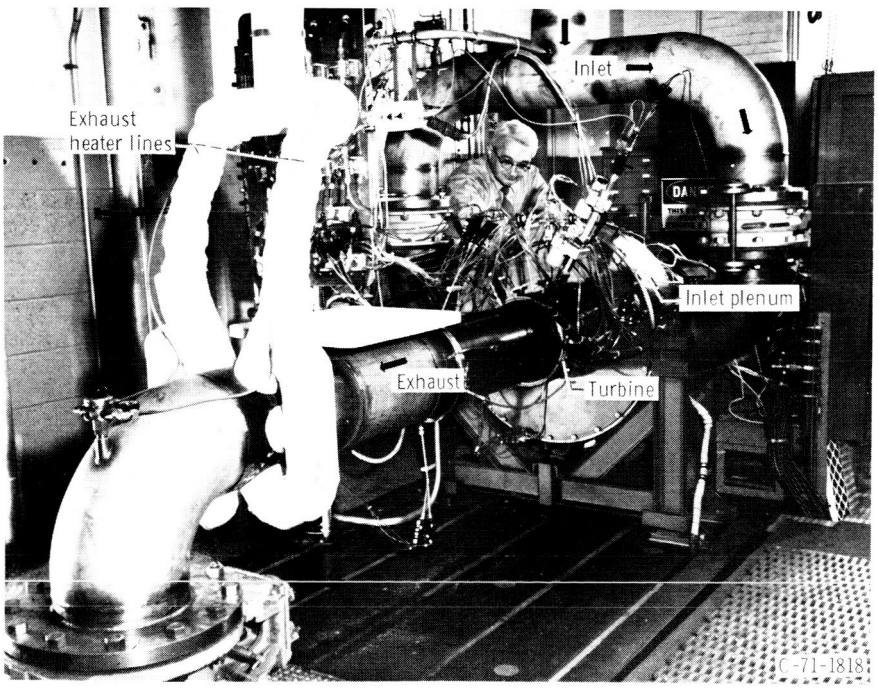

(b) Turbine test apparatus.

Figure 7. - Experiment equipment.

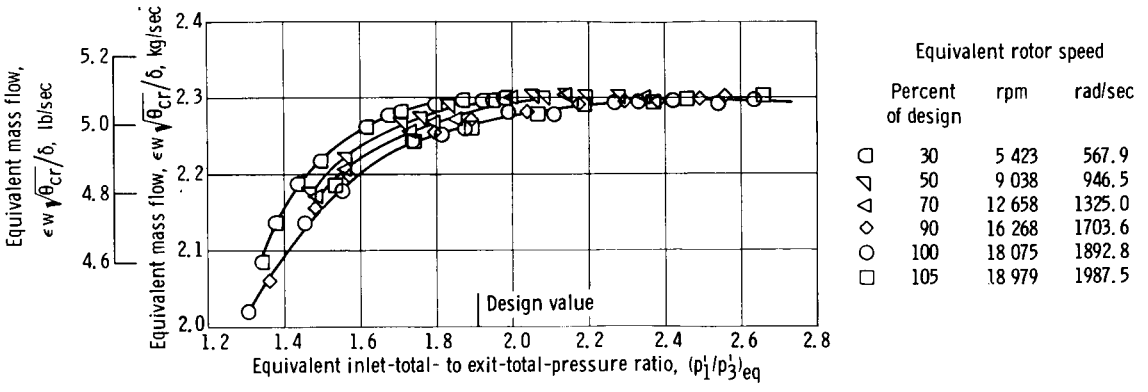

Figure 8. - Variation of mass flow with total-pressure ratio and speed.

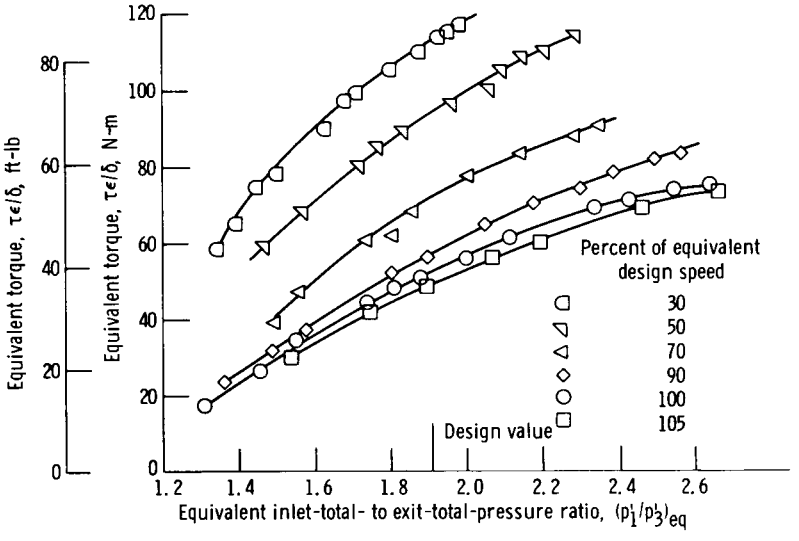

Figure 9. - Variation of torque with pressure ratio and speed.

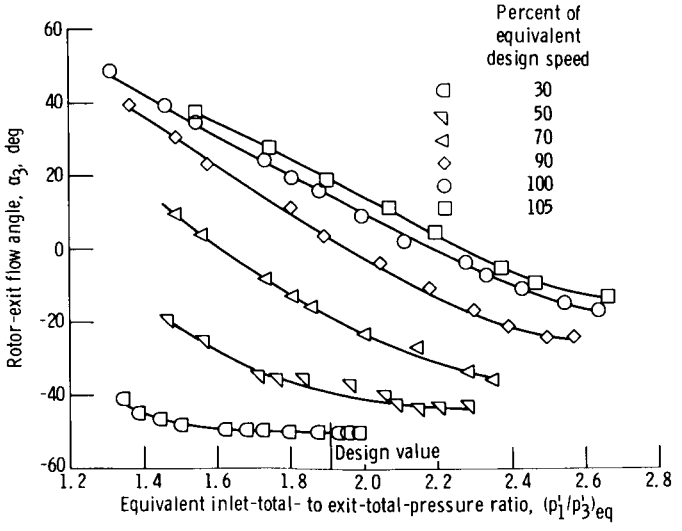

Figure 10. - Variation of rotor-exit flow angle (at mean radius) with pressure ratio and speed.

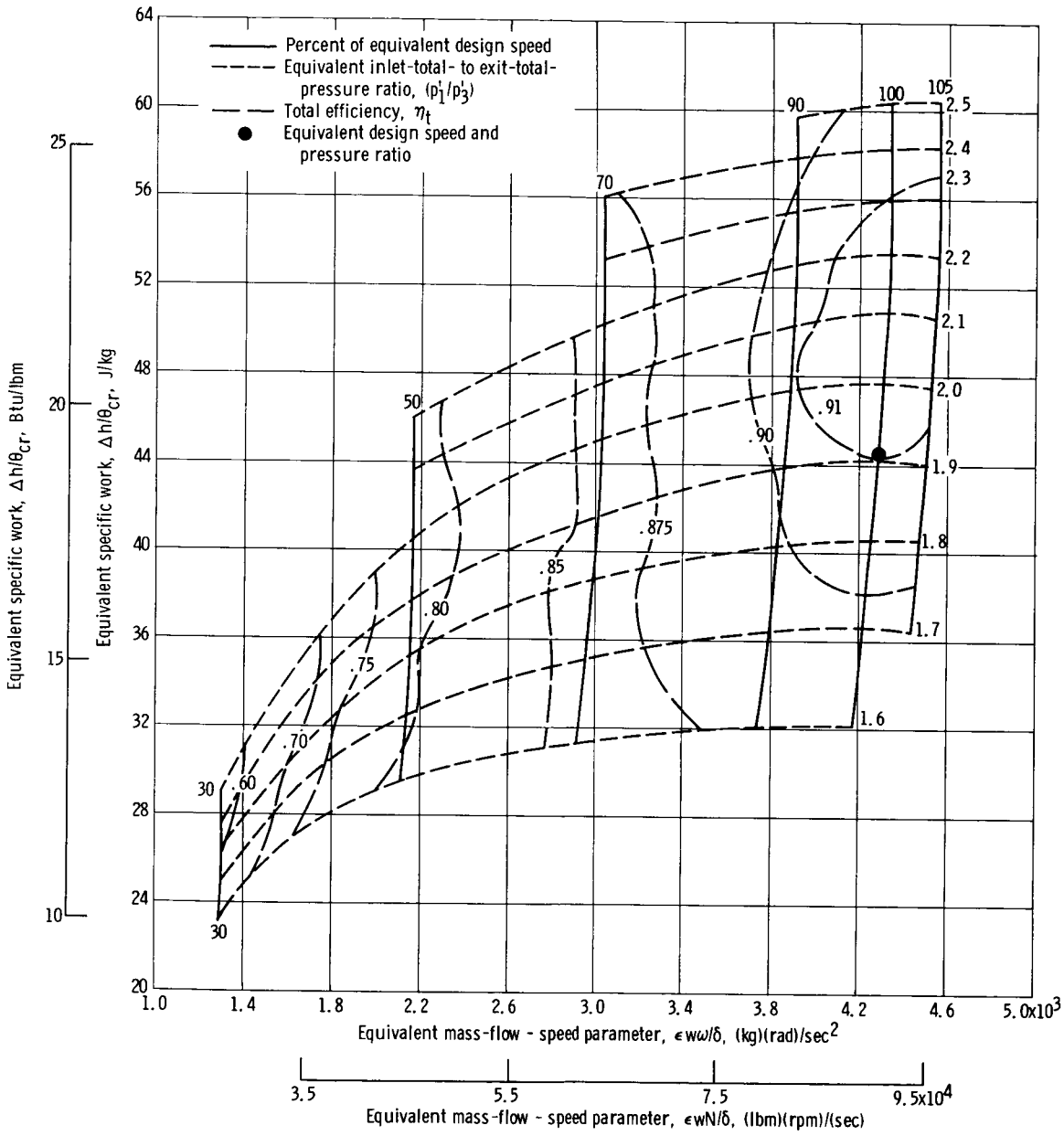

(a) Total efficiency.

Figure 11. - Overall turbine performance map.

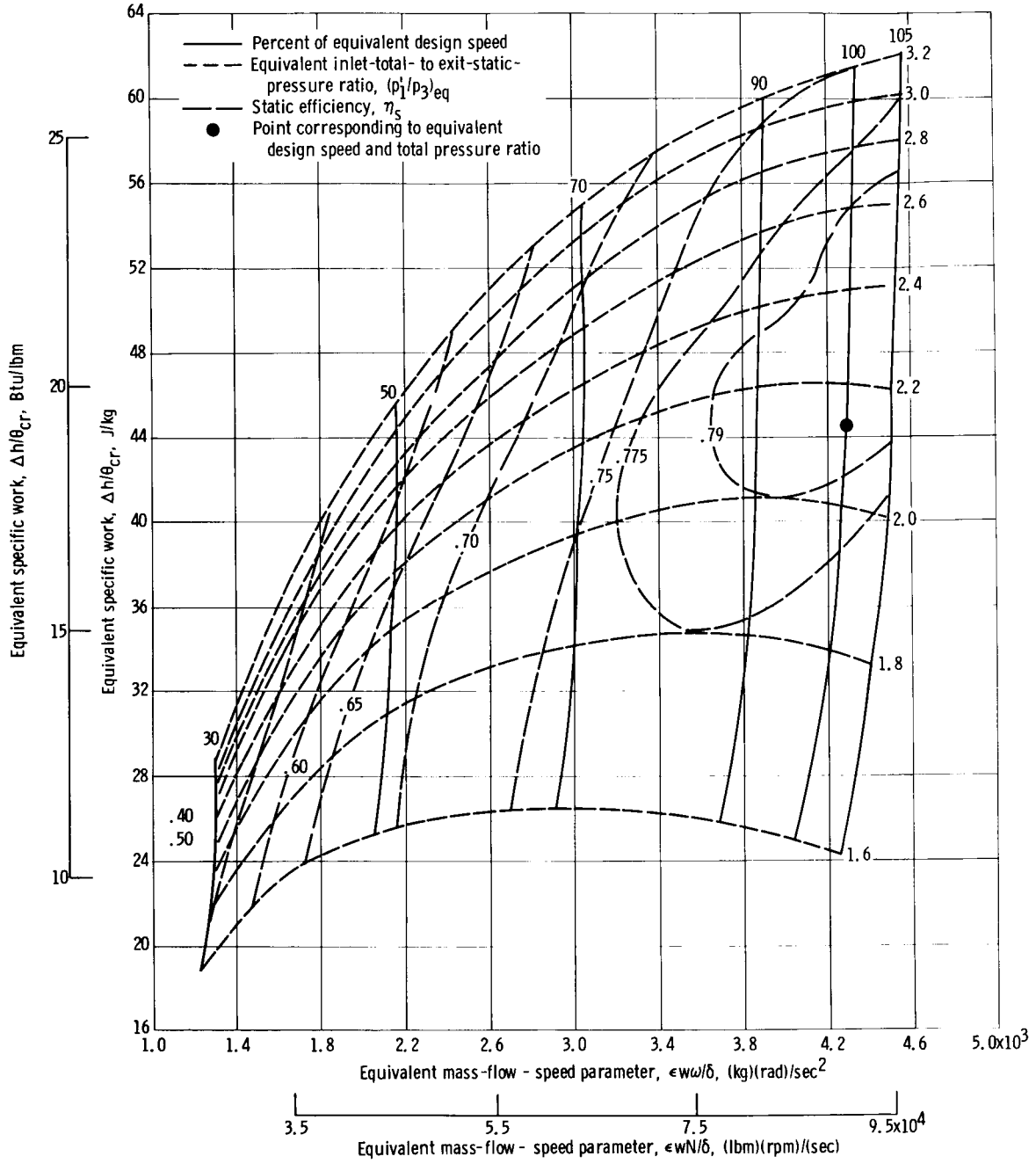

(b) Static efficiency.

Figure 11. - Concluded.

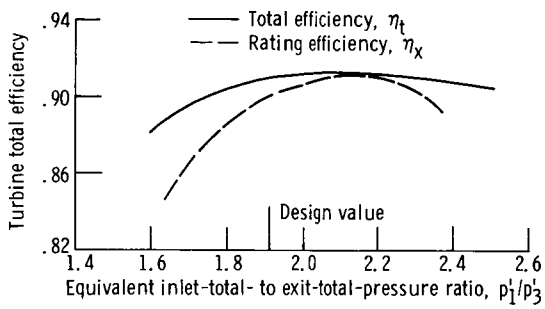

Figure 12. - Comparison of total efficiency with rating efficiency at equivalent design speed and over range of total-pressure ratio.

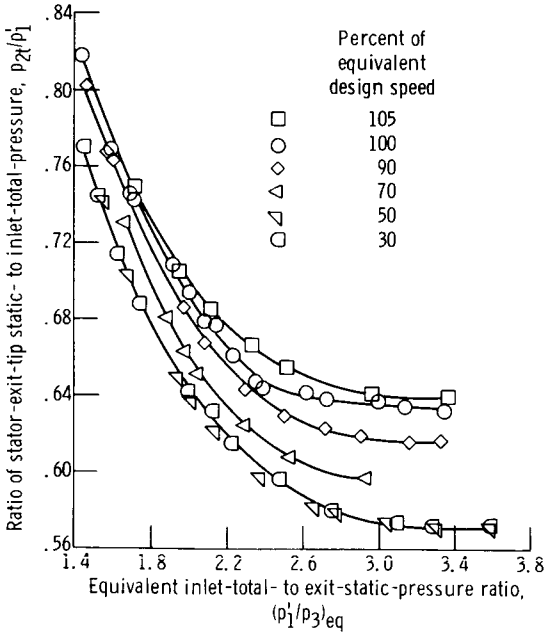

Figure 13. - Variation of stator-exit-tip static-pressure with pressure ratio and speed.

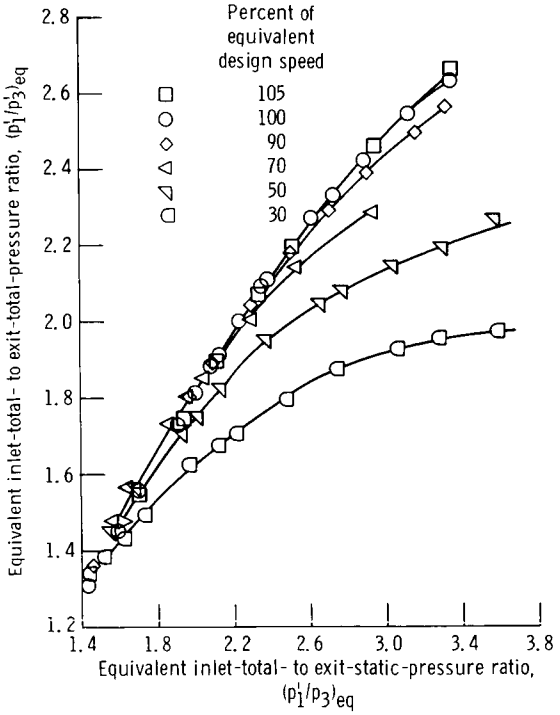

Figure 14. - Variation of total-pressure ratio with static-pressure ratio and speed.